

The Interaction Between Slag and MgO Refractory at Conditions Relevant to Nickel Laterite Ore Smelting

Y.H. Putra¹, Z. Zulhan², A.D. Pradana³, D.R. Pradana⁴ and T. Hidayat⁵

1. Currently: Junior Business Analyst, PT Bukit Asam, Tanjung Enim, South Sumatera 31716, Indonesia. Email: yudhithp.13@gmail.com
Previously: Researcher, Metallurgical Engineering Research Group, Faculty of Mining and Petroleum Engineering, Bandung Institute of Technology, Bandung, West Java 40132, Indonesia.
2. Professor, Metallurgical Engineering Research Group, Faculty of Mining and Petroleum Engineering, Bandung Institute of Technology, Bandung, West Java 40132, Indonesia. Email: zulfiadi.zulhan@itb.ac.id
3. Business Development Manager, PT Gunbuster Nickel Industry, Indonesia Stock Exchange Building Tower I, 31st Floor, Unit 3101, Jakarta 12190, Indonesia. Email: gika@bharuna.com
4. Operation Supervisor, PT Gunbuster Nickel Industry, Indonesia Stock Exchange Building Tower I, 31st Floor, Unit 3101, Jakarta 12190, Indonesia. Email: dimas@efi.co.id
5. Lecturer, Metallurgical Engineering Research Group, Faculty of Mining and Petroleum Engineering, Bandung Institute of Technology, Bandung, West Java 40132, Indonesia. Email: t.hidayat@itb.ac.id

Keywords: Nickel Laterite Ore Smelting, Slag, Magnesia Refractory, Refractory-Melt Interaction.

ABSTRACT

The high temperature processing of nickel laterite ore is currently dominated by the Rotary Kiln-Electric Furnace (RKEF) technology. The ratio of SiO_2/MgO (S/M) in the ore is one of the critical parameters that determines the success of the RKEF process. Incompatible S/M ratios in the ore can cause aggressive chemical interaction between the slag and MgO refractory. The slag-refractory interaction at conditions relevant to nickel laterite ore smelting was investigated in the present study. Synthetic mixtures representing the slag compositions of nickel laterite ore smelting were prepared by mixing MgO, SiO_2 , Al_2O_3 , CaO, Fe_2O_3 , and Fe and heating the mixtures in steel containers at 1300°C under an argon atmosphere for 3 hours. Pure MgO crucible were used as containment material in the melting process of the mixtures to represent the MgO refractory. The kinetics of the slag-refractory reaction were investigated using samples with selected initial S/M ratios of 2.0 and 3.0 (wt./wt.) (with constant CaO = 3 wt.%, Al_2O_3 = 5 wt.%, FeO = 10wt.%) by performing melting at 1500°C in MgO crucibles for 5, 30, and 120 minutes under an argon atmosphere. The effect of the S/M ratio in slag on the slag-refractory interaction was also investigated by performing melting of mixtures with different initial S/M ratios of 1.75, 2.0, 2.5, and 3.0 (wt./wt.) in MgO crucibles at 1500°C for 120 minutes under an argon atmosphere. After the melting process, each sample was quenched in water, mounted in resin, ground, polished, and coated. The interaction between the slags and MgO refractory was then evaluated by analysing the polished samples using a scanning electron microscope equipped with an energy dispersive spectroscopy (SEM-EDS). Thermodynamic simulations using FactSage 8.0 thermochemical software were performed based on the experimental slag compositions, refractory, and conditions to support the evaluation process. The results show that a higher S/M ratio in slag leads to a higher tendency for the refractory component to dissolve into the slag. A higher S/M ratio in slag also leads to an increasing extent of solid-state diffusion of iron oxide into the remaining refractory grains. The dissolution of MgO into the slag is rapid; the MgO concentration in the final slag increased by 2.4 wt.% and 5.7 wt.% at initial S/M ratios of 2.0 and 3.0 wt./wt., respectively, within 5 and 30 minutes of the melting process.

INTRODUCTION

The Rotary Kiln – Electric Furnace (RKEF) technology is commonly employed for the production of ferronickel (FeNi) or nickel pig iron (NPI), with nickel and iron contents ranging from 10-30% and 70-90% respectively (Crundwell *et al* 2011). The simplified flowsheet of RKEF process is provided in FIG 1. The RKEF process involves three primary stages in processing nickel ore. The initial stage entails drying the ore in a rotary dryer at 250°C , which serves to decrease the water content from 30% to 20%. Subsequently, the ore undergoes calcination in a rotary kiln at temperatures between $750\text{-}900^\circ\text{C}$, during which remaining water content is removed and the nickel oxide and iron oxide are partially reduced by the reductant. The resulting calcine, which is the product from the rotary kiln, is then smelted in an electric furnace at temperatures ranging from $1450\text{-}1550^\circ\text{C}$ in order to form and separate the metal product from the slag. In a few RKEF plants, an additional purification step may be carried out using a ladle furnace to reduce impurity content in the final product.

The electric furnace is a widely employed smelting technology in various metal industries. It operates on the principle of resistance heating, where the burden materials such as calcine, slag, and molten metal are heated through the application of electric current (Degel *et al* 2007). To withstand the high temperatures and harsh conditions within the furnace, refractory materials are used for lining purposes. In the nickel industry, magnesia (MgO) refractory is utilized as a lining for the electric furnace. This choice is due to the high melting point of magnesia, its favorable mechanical properties at elevated temperatures, and its resistance to adverse environments. However, there are a few disadvantages of using MgO refractory, such as it has a very high conductivity, which can result in significant heat loss during the smelting process (Ruh and McDowell 1962) and it has a relatively high thermal expansion compared to other types of refractories (Gangler 1950).

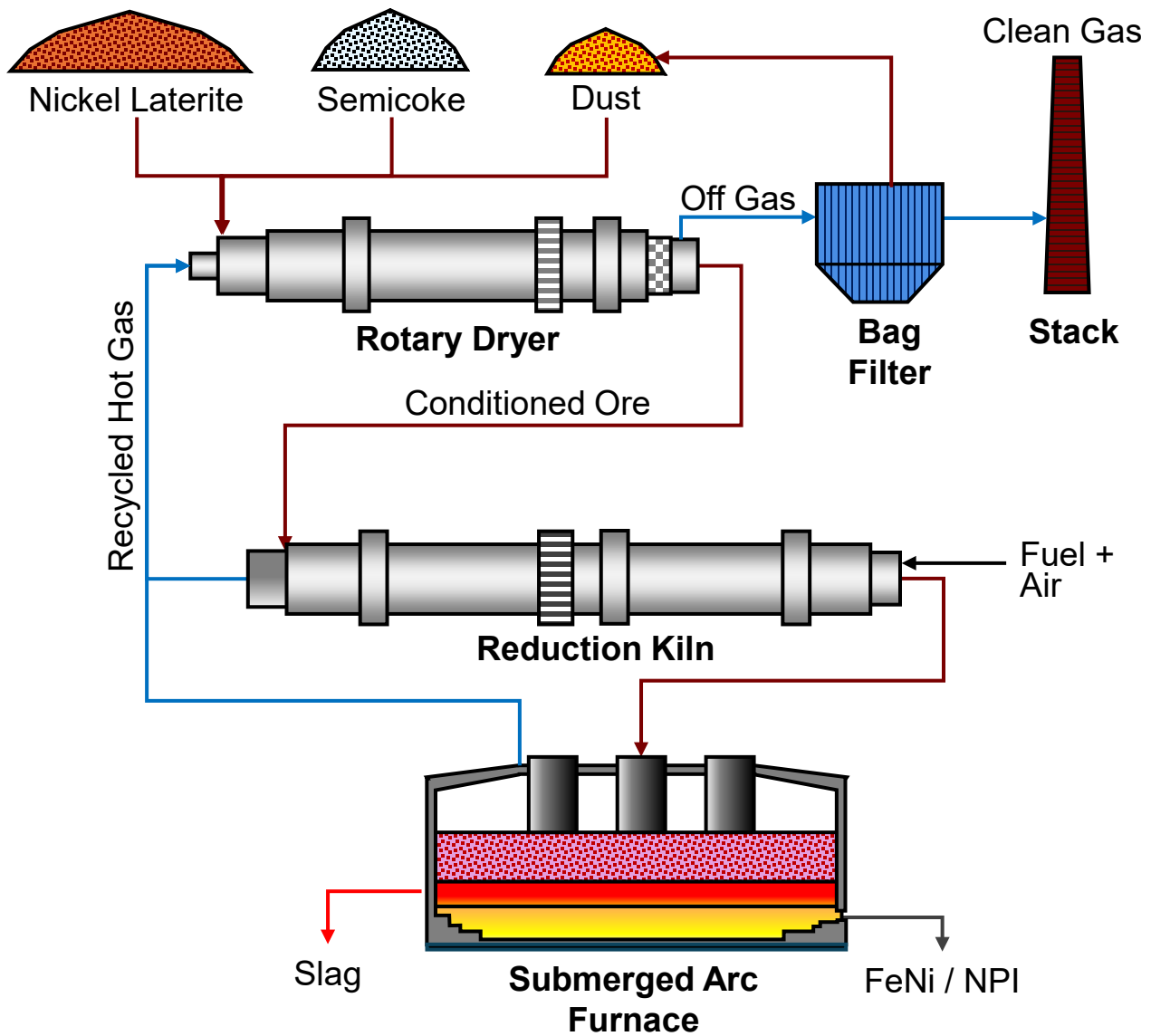


FIG 1 – Simplified flowsheet of RKEF process

The malfunction of refractory material not only leads to a loss of productivity but also poses risks to the surrounding environment (Zhang and Lee 2013). Consequently, the investigation of the interaction between slag and refractories has garnered significant attention from researchers (Huang *et al* 2017; Sagadin *et al* 2016; Sagadin *et al* 2017; Sagadin *et al* 2018; Sagadin *et al* 2018b; Sagadin *et al* 2021; Wagner *et al* 2016) within the nickel industry. Generally, refractory damage can be attributed to three primary factors: chemical attack, thermal pressure, and mechanical pressure. Among these, chemical attack predominantly occurs as a result of the chemical interaction between the refractory and slag. In a number of electric furnaces, water-cooling components are incorporated into the lining structure to absorb heat. This facilitates the formation of a thin freeze lining, which serves to protect the refractories from corrosion caused by the slag (Kotzé 2002). While in some of electric furnaces, the water-cooling components are not available, hence the furnace integrity relies heavily on the chemical interaction between slag and refractory material. This study aims to investigate the slag and refractory interaction under conditions relevant to ferronickel or NPI smelting as a function of initial SiO_2/MgO ratio in slag and melting time. Synthetic slag was used to replicate the industrial slag and a dense pure MgO crucible was used to simulate the actual refractory material. The use of a dense MgO crucible eliminates the effects of physical infiltration of slag due to the heterogeneity and porosity commonly found in the refractory material, thus focusing the investigation mainly on the chemical attack of slag on the refractory material.

EXPERIMENTAL

Preparation and Characterization of Synthetic Slag

The synthetic slag used in this experiment was produced by mixing high purity reagents, including MgO, SiO₂, Al₂O₃, CaO, Fe₂O₃, and Fe. These reagents were then blended with specific compositions to achieve constant FeO, Al₂O₃, and CaO contents of 10%, 5%, and 3%, respectively, in the slag. The chosen compositions were based on typical slag compositions in one of the ferronickel or NPI plants. As for the SiO₂ and MgO, their compositions were adjusted so that the final SiO₂/MgO or S/M ratios were set around 1.75, 2.0, 2.5, and 3.0. The reagents were mixed and homogenized using a mortar for 10 minutes. The resulting mixtures were then placed in cylindrical stainless steel 304 crucibles with dimension of 20 mm in diameter and 60 mm in height. The crucibles were then positioned on an alumina boat to enable heating using a horizontal tube furnace. The synthetic slags were heated in the horizontal tube furnace at a temperature of 1300°C, aimed at pre-reacting the oxides within the synthetic slags before melting them with the MgO crucible. The synthetic slags obtained from the heating in the horizontal tube furnace were then homogenized again using a mortar for 10 minutes. The compositions of the synthetic slags with different S/M ratios were checked using SEM-EDS. The results of the SEM-EDS semi-quantitative analysis for all samples are presented in TABLE 1.

TABLE 1 – Semi-quantitative EDS-measured composition of synthetic slag

Target S/M	Composition (wt. %)					
	SiO ₂	MgO	FeO	Al ₂ O ₃	CaO	S/M
1.75	51.9	31.1	8.9	5.4	2.6	1.67
2.0	56.2	27.2	8.6	4.8	2.9	2.07
2.5	60.4	24.2	8.6	4.4	2.4	2.50
3	62.4	21.0	10.1	4.0	2.5	2.97

Melting in Vertical Tube Furnace

There are several experimental methods commonly used to study the slag-refractory interaction, including: (i) Button or sensible drop test; (ii) Dipping, immersion, or finger test; (iii) Crucible, cavity, cup, or brick; (iv) Induction furnace test; (v) Rotating finger test; and (vi) Rotating slag test (Zhang and Lee 2004). The interaction between slag and refractory in this study was conducted using the cup test technique. This technique is easier to implement and ensures that the entire slag interacts with the refractory compared to other techniques, such as the finger test. However, this technique also has limitations, such as the inability to study the corrosion effects of fluid movement and the tendency of slag samples to become saturated due to the significantly smaller proportion of slag compared to the refractory. In industrial settings, the proportion of slag should be much larger than that of the refractory. The synthetic slag was weighed at 1.3 grams and then placed into the MgO crucible. The MgO crucible with dimension of 16 mm in diameter and 20 mm in height was used. The fusion of synthetic slag with the MgO refractory was carried out using a vertical tube furnace. The sample was suspended using molybdenum wire and held within the hot zone of the furnace under argon atmosphere at 1500°C for 5, 30, and 120 minutes. After melting, the samples were rapidly quenched in water.

Product Preparation and Examination

The quenched samples were dried and embedded in resin to prevent them from breaking during the sample preparation process. The samples were then cut in half at their midsection using a ceramic cutter, remounted in resin, and polished using an automated polishing device. The polished samples obtained from the experiments were examined using an optical microscope (Jiangxi Phoenix L2030A Trinocular Microscope) and semi-quantitatively analyzed using scanning electron microscope with energy dispersive spectroscopy (SEM-EDS, JEOL NeoScope JCM-7000). The semi-quantitative SEM-EDS analysis was conducted at the refractory-slag interface at 12 different locations distributed

approximately 0.5 mm towards the refractory and 0.5 mm towards the slag, as shown in FIG 2. Various reference materials were used to validate the accuracy of the compositional analysis by the EDS detector. The reference materials used in the present measurement were Basaltic glass (NMNH 113498-1) and Springwater Olivine (USNM 2566) of the Smithsonian Microbeam Standards obtained from the Smithsonian National Museum of Natural History, USA. It was observed that the compositions measured by EDS were within a deviation of less than 1.4% by weight compared to those reported in the reference certificates.

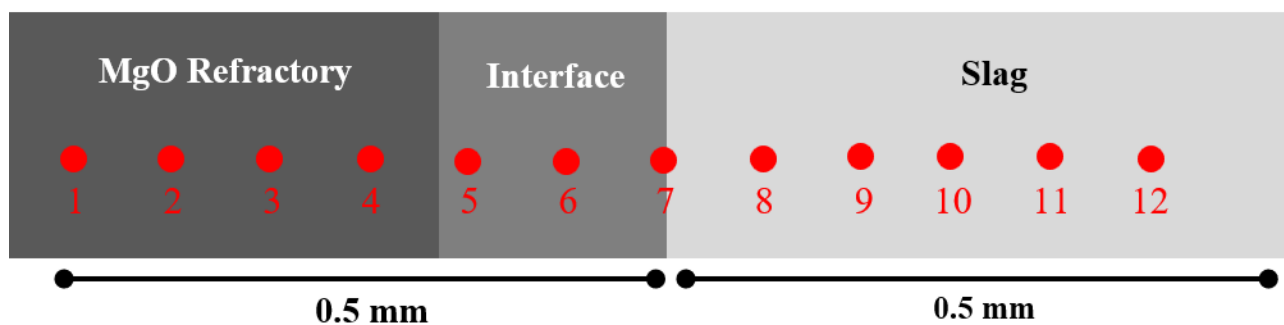


FIG 2 – Illustration of semi-quantitative analysis of composition along refractory and slag interface

RESULTS AND DISCUSSION

The Reaction Kinetics of MgO Dissolution from MgO Refractory into Slag

The kinetics of MgO dissolution from the refractory into the slag were investigated at a temperature of 1500°C using synthetic slags with initial SiO₂/MgO (S/M) ratios of 2.00 and 3.00, with melting times varied between 5, 30, and 120 minutes. An example of secondary electron image from kinetic experiments using a mixture with an initial S/M ratio of 3.00 reacted at 1500°C can be seen in FIG 3. After melting for 5 minutes, the sample shows both slag and several solid particles (see FIG 3(a)). The solid particles appear to be part of oxides from the initial synthetic slag mixture, which are in the process of dissolving into the liquid slag phase. A fully liquid slag is observed after melting for 30 minutes (see FIG 3(b)). After 120 minutes of melting, slag along with olivine is observed (see FIG 3(c)). It is worth noting that the surface of the MgO refractory appears relatively smooth after melting for 5 and 30 minutes compared to after 120 minutes of melting. The relatively smooth MgO surface indicates the ongoing dissolution process of solid MgO into the liquid slag.



FIG 3 – Examples of secondary electron images from samples melted at 1500°C with an initial SiO₂/MgO ratio in slag of 3.00 for melting times of: (a) 5 minutes; (b) 30 minutes; and (c) 120 minutes

The semi-quantitative EDS measured compositions of the samples along refractory and slag interface from kinetic experiments using samples with initial S/M ratios of 2.00 and 3.00 are provided in TABLE 2 and TABLE 3, respectively. The compositions of the dominant components, i.e., MgO, SiO₂, and FeO, are plotted in FIG 4 and FIG 5. The dissolution of MgO appears to be rapid so that

after the reaction continued from 5 minutes to 30 minutes, the MgO concentration in slag increased significantly, approaching the MgO concentration from melting for 120 minutes. On the other hand, SiO₂ concentration in slag continuously decreases due to dilution by the dissolving MgO. There appears to be no clear trend regarding FeO concentration in slag with melting time. In the case of the MgO refractory composition, it appears to remain unchanged in most of experiments, except for the experiment using a sample with an initial S/M ratio in slag of 3.00 and a melting time of 120 minutes, which showed a significant increase in FeO concentration within the refractory.

The bulk compositions of liquid slag (the compositions of liquid slag at the furthest position from the refractory, i.e. at point 12) from the kinetic experiments using samples with initial S/M ratios in slag of 2.00 and 3.00 are provided in FIG 6(a) and FIG 6(b), respectively. The increasing MgO and decreasing SiO₂ in the slag can be seen clearly in both figures. Both of these lead to an increasing S/M ratio in the final liquid slag with increasing melting time, as shown in FIG 6(c). The dissolution of MgO is rapid, so as the reaction proceeds from 5 minutes to 30 minutes, the MgO concentration in the slag increases significantly by 2.4 wt.% and 5.7 wt.% for initial S/M ratios of 2.0 and 3.0 wt./wt., respectively. However, when the reaction proceeds from 30 minutes to 120 minutes, the dissolution of MgO is less rapid and approaches completion. The slowdown in the dissolution of MgO is possibly due to the reduced driving force for the MgO dissolution as the liquid approaches MgO saturation condition, which later can lead to the formation of olivine precipitates on the MgO surface.

TABLE 2 – Semi-quantitative EDS measured composition along refractory-slag interface from samples melted at 1500°C with an initial SiO₂/MgO ratio in slag of 2.00 for melting times between 5 and 120 minutes

Sample	Position												
	1	2	3	4	5	6	7	8	9	10	11	12	
t=5min	MgO	98.6	98.9	98.2	99.0	98.7	98.6	87.8	30.6	30.3	24.7	24.8	26.9
	SiO ₂	0.7	0.6	0.4	0.3	0.3	0.5	0.7	53.5	51.7	56.1	56.3	55.3
	Al ₂ O ₃	0.3	0.3	0.4	0.3	0.5	0.4	2.3	2.7	5.1	5.2	5.6	5.3
	CaO	0.2	0.1	0.7	0.2	0.1	0.1	0.3	1.5	2.5	2.6	2.7	2.6
	FeO	0.2	0.2	0.5	0.1	0.4	0.4	8.9	11.7	10.4	11.4	10.7	10.0
t=30min	MgO	98.9	99.0	98.7	98.4	97.9	95.7	82.9	45.3	37.3	30.6	31.8	29.3
	SiO ₂	0.4	0.3	0.3	0.7	0.6	0.8	1.1	45.7	48.4	51.0	50.4	52.3
	Al ₂ O ₃	0.5	0.5	0.5	0.4	0.4	0.6	0.3	0.9	3.6	5.2	4.9	5.1
	CaO	0.1	0.0	0.1	0.2	0.1	0.2	0.2	0.4	1.6	2.7	2.1	2.6
	FeO	0.2	0.2	0.5	0.3	1.1	2.7	15.5	7.7	9.1	10.5	10.8	10.8
t=120min	MgO	98.6	98.1	98.1	96.4	95.5	92.3	54.3	37.8	34.0	32.4	32.3	31.4
	SiO ₂	0.3	0.3	0.3	0.8	0.3	0.5	42.0	50.7	49.1	48.4	49.5	52.0
	Al ₂ O ₃	0.4	0.3	0.5	0.6	0.7	1.1	1.5	3.3	5.5	6.5	6.0	4.5
	CaO	0.0	0.1	0.0	0.0	0.0	0.1	0.1	1.3	2.5	3.4	3.1	3.2
	FeO	0.6	1.2	1.1	2.2	3.4	6.0	2.1	6.9	8.9	9.4	9.1	8.9
REFRACTORY							OLIVINE		SLAG				

TABLE 3 – Semi-quantitative EDS measured composition along refractory-slag interface from samples melted at 1500°C with an initial SiO₂/MgO ratio in slag of 3.00 for melting times between 5 and 120 minutes

Sample	Position												
	1	2	3	4	5	6	7	8	9	10	11	12	
t=5min	MgO	98.8	97.6	98.8	98.6	97.6	96.4	85.9	26.5	26.7	26.5	26.0	24.2
	SiO ₂	0.6	1.0	0.6	0.6	1.2	1.2	1.7	58.1	59.4	59.8	60.5	59.5
	Al ₂ O ₃	0.5	0.7	0.4	0.6	0.6	0.5	0.8	4.0	3.5	3.8	4.0	4.2
	CaO	0.2	0.3	0.1	0.1	0.2	0.3	1.9	2.8	2.4	2.3	2.4	2.9
	FeO	0.0	0.3	0.2	0.1	0.5	1.6	9.8	8.6	8.0	7.7	7.1	9.2
t=30min	MgO	98.5	98.8	98.1	97.9	97.2	94.3	67.6	39.1	30.7	27.4	31.0	29.9
	SiO ₂	0.1	0.3	0.8	0.5	0.5	1.2	6.0	50.2	54.8	56.9	54.6	55.7
	Al ₂ O ₃	0.5	0.6	0.6	0.6	0.6	0.6	2.2	1.5	3.4	3.9	4.0	4.2
	CaO	0.0	0.1	0.1	0.1	0.1	0.2	0.2	0.7	2.0	2.4	2.0	2.2
	FeO	0.8	0.3	0.4	0.9	1.6	3.7	24.1	8.5	9.2	9.4	8.4	8.0
t=120min	MgO	84.1	84.8	84.7	79.3	65.4	68.6	46.0	41.1	40.1	31.2	30.9	28.9
	SiO ₂	3.7	1.0	1.3	1.4	6.5	2.2	32.6	46.0	46.6	50.2	51.4	52.5
	Al ₂ O ₃	3.0	1.0	0.6	1.1	1.6	1.4	4.9	4.2	4.1	6.5	5.1	5.9
	CaO	0.9	0.6	0.5	0.8	3.5	0.8	2.5	2.1	1.8	3.3	2.4	2.6
	FeO	8.4	12.6	13.0	17.4	23.1	27.0	14.0	6.6	7.4	8.8	10.3	10.3
REFRACTORY							OLIVINE		SLAG				

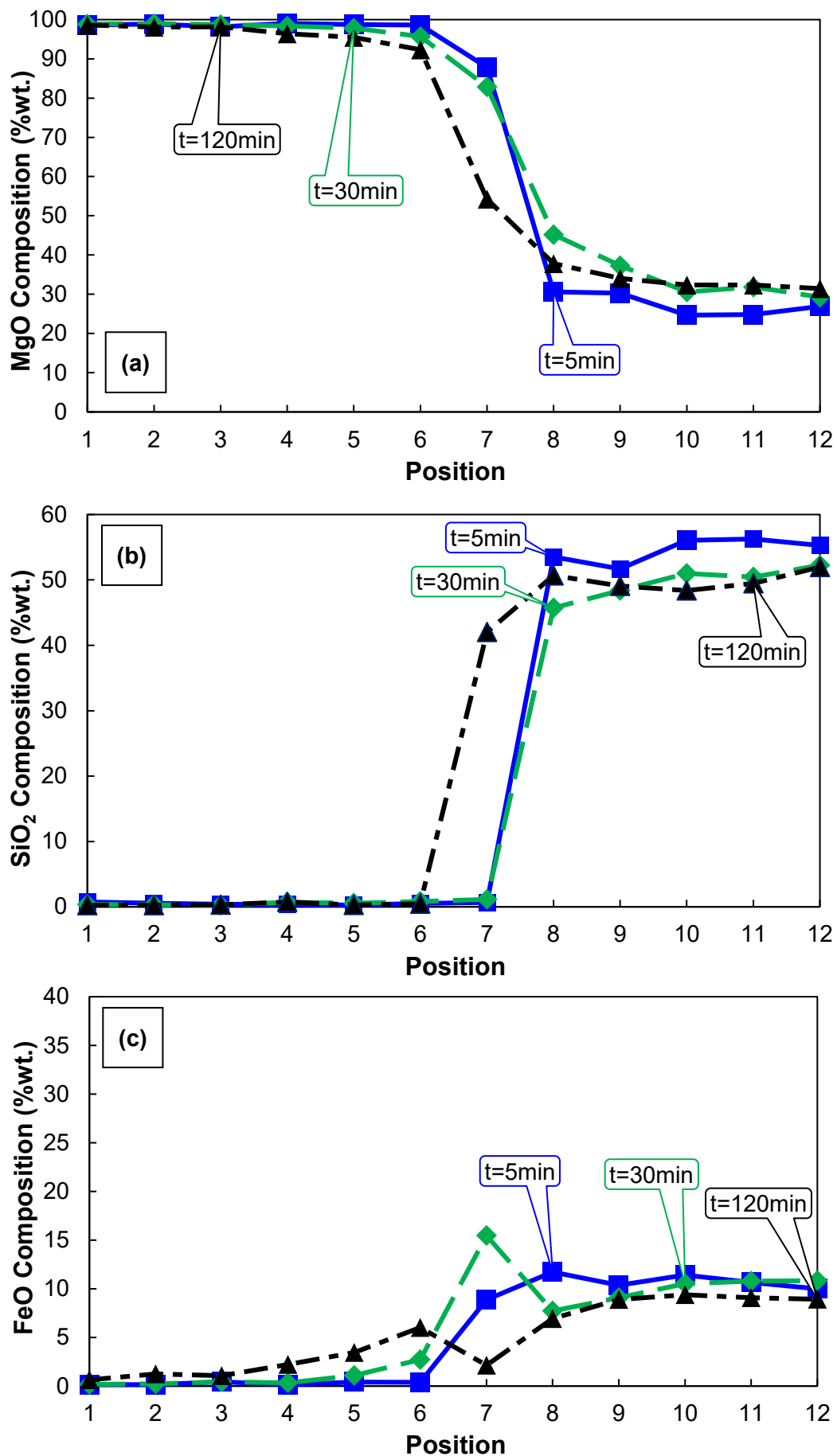


FIG 4 – Semi-quantitative compositional analysis along refractory-slag interface from samples melted at 1500°C with an initial SiO₂/MgO in slag ratio of 2.00 for melting time between 5 and 120 minutes: (a) MgO composition; (b) SiO₂ composition; and (d) FeO composition

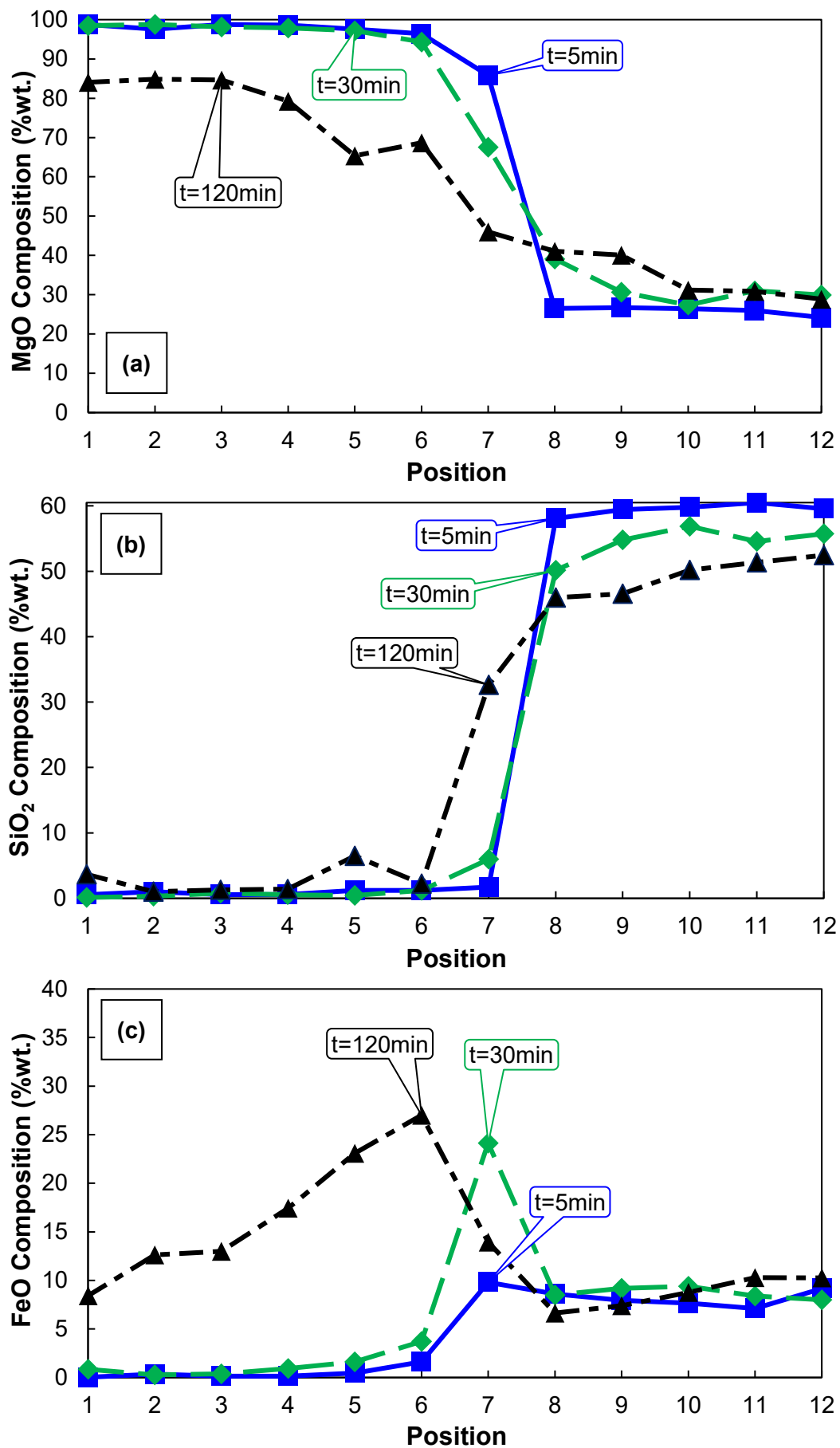


FIG 5 – Semi-quantitative compositional analysis along refractory-slag interface from samples melted at 1500°C with an initial SiO₂/MgO ratio in slag of 3.00 for melting time between 5 and 120 minutes: (a) MgO composition; (b) SiO₂ composition; and (d) FeO composition

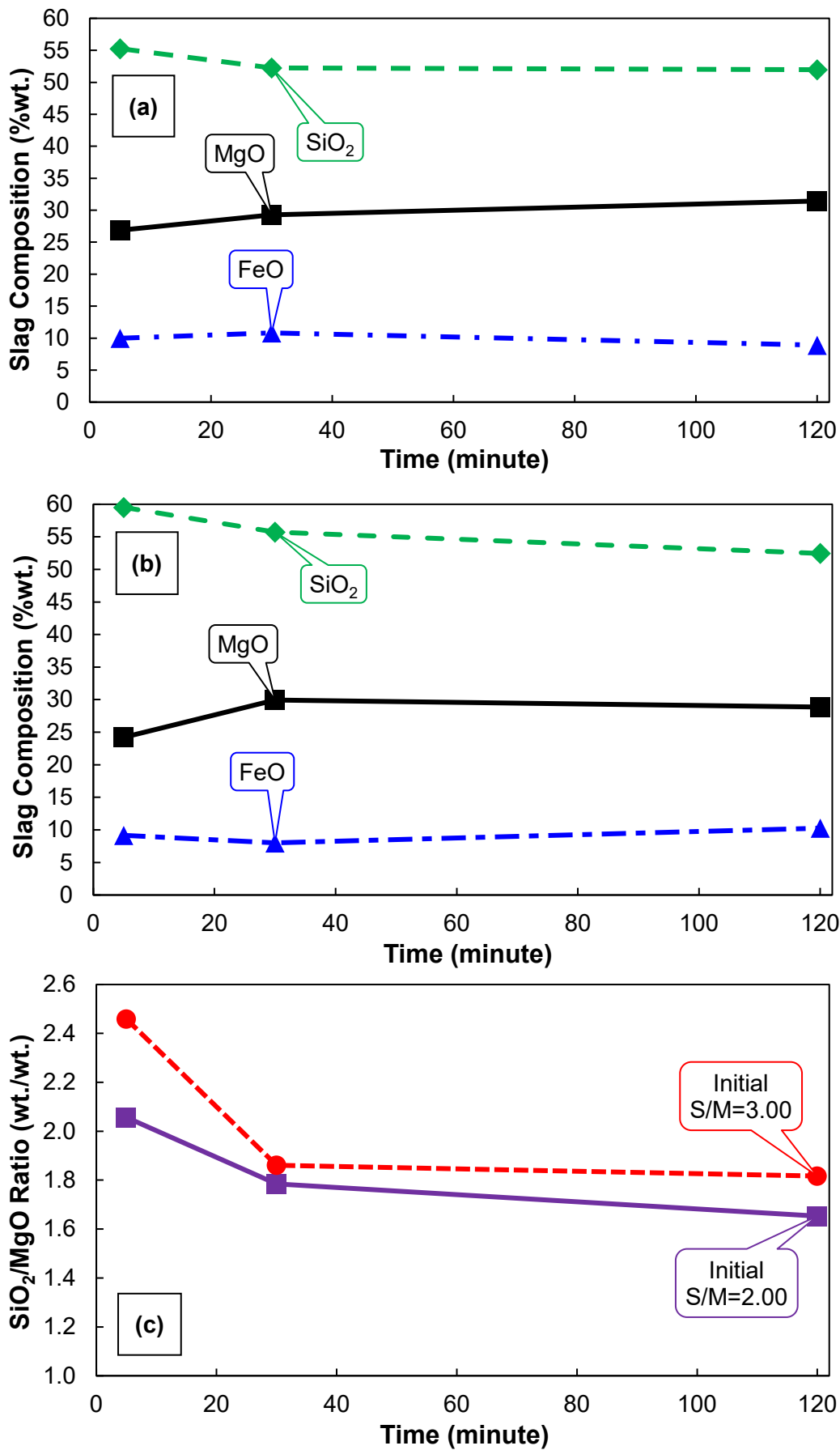


FIG 6 – Bulk composition of liquid slag from semi-quantitative compositional analysis of samples melted at 1500°C for melting time between 5 and 120 minutes: (a) Sample having initial SiO₂/MgO ratio in slag of 2.00; (b) Sample having initial SiO₂/MgO ratio in slag of 3.00; and (d) SiO₂/MgO ratio in the final slag

The pseudo-ternary diagram MgO-FeO-SiO₂, at constant CaO content of 3 wt.% and Al₂O₃ content of 5 wt.%, relevant to the slag system in the present study, is shown in FIG 7. The diagram was calculated using FactSage 8.2 (Bale *et al* 2011) with the liquid Fe activity set to 0.9, corresponding to the activity of iron in the NPI metal. The initial slag compositions for samples with initial S/M ratios in slag of 2.00 and 3.00 are plotted in the figure. Additionally, the slag compositions from samples melted at 1500°C with initial S/M ratios in slag of 2.00 and 3.00 for melting times of 5 minutes, 30 minutes, and 120 minutes are also included in the figure. Contacting the mixtures with MgO refractory at 1500°C results in the movement of the liquid slag composition toward the MgO corner of the ternary diagram. Theoretically the movement of the liquid slag should conclude at the liquidus of olivine for 1500°C, where the liquid slag is saturated by MgO and olivine solid is formed. However, the measured liquid slag composition extends beyond the 1500°C liquidus. This discrepancy may arise due to several reasons, including inaccurate liquids prediction by FactSage due to an unoptimized database, inaccuracy in temperature setup during melting experiments, inclusion of olivine solid in the measurement of liquid slag composition, or chemical segregation of the liquid slag during cooling which results in the measured slag composition not accurately representing its actual composition at high temperature.

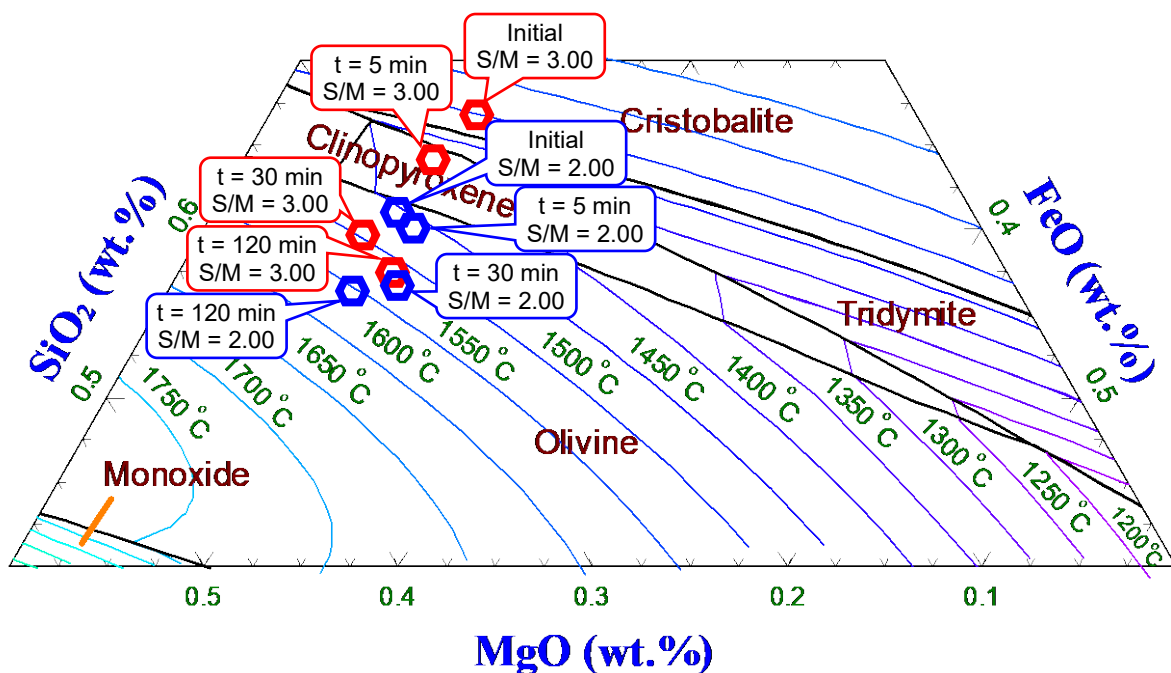


FIG 7 – FactSage calculated pseudo-ternary diagram of MgO-FeO-SiO₂ at CaO = 3 wt.% and Al₂O₃ = 5 wt.% in equilibrium with liquid Fe ($\alpha_{Fe} = 0.9$)

The Effect of SiO₂/MgO Ratio in the Initial Slag on The Interaction between Slag and MgO Refractory

The effect of initial slag composition on the interaction between slag and MgO refractory was investigated by conducting melting of samples with initial SiO₂/MgO (S/M) ratios in slag of 1.75, 2.00, 2.50, and 3.00 at 1500°C. A melting time of 120 minutes was selected to ensure that the interaction between slag and refractory approaches completion, as demonstrated by the melting time variation experiments. Moreover, the 120 minutes melting time was chosen since it closely resembles the residence time of melts in the electric furnace in the industrial practice. The secondary electron image and elemental mapping of the melted samples with various initial S/M ratios in slag at 1500°C are provided in FIG 8.

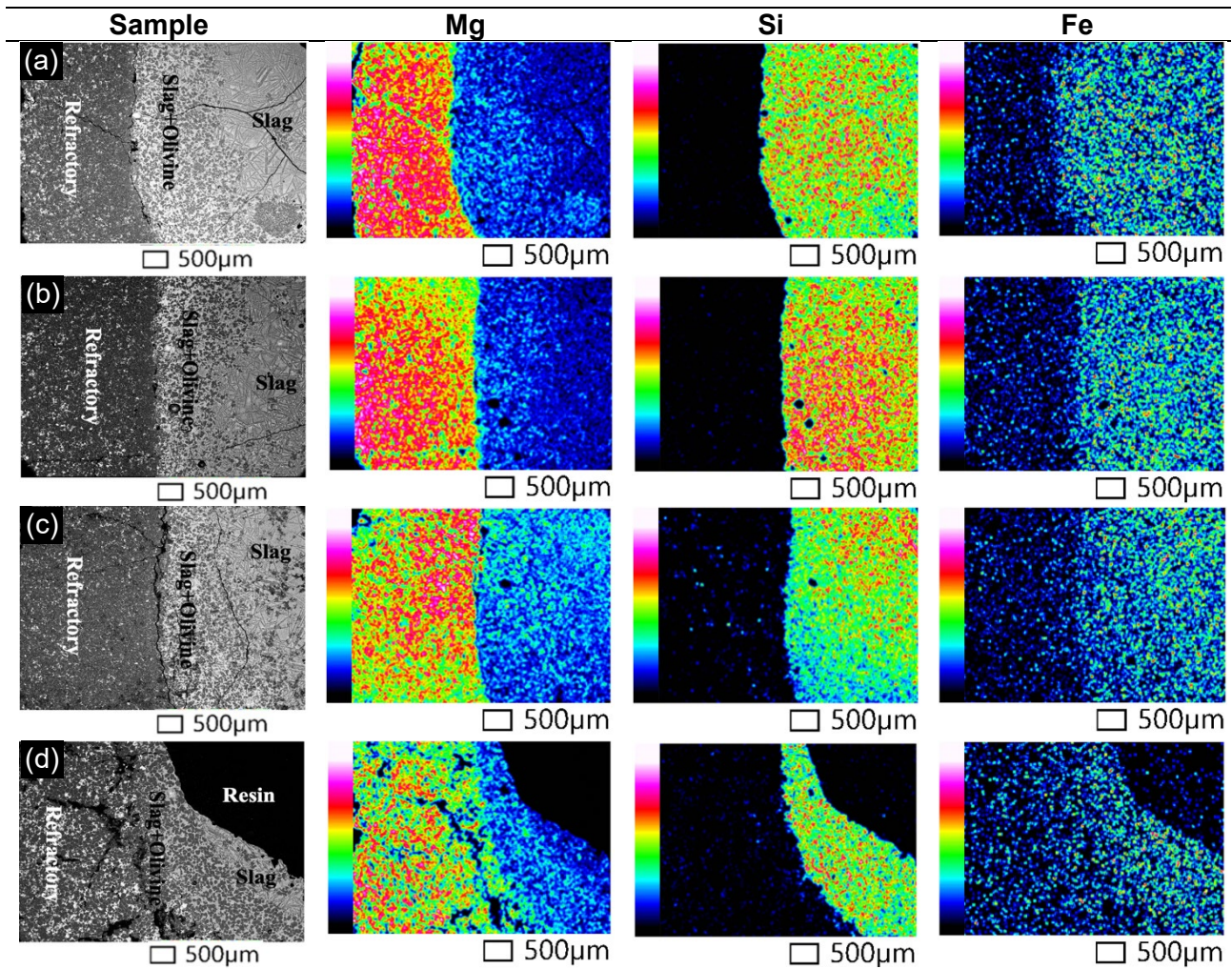


FIG 8 – Secondary electron image and elemental mapping from samples melted at 1500°C for melting time of 120 minutes with initial SiO₂/MgO ratios in slag of: (a) 1.75; (b) 2.00; (c) 2.50; and (d) 3.00

All samples exhibit areas of slag, slag-olivine mixture, and dense MgO. The sample with an initial S/M ratio of 3.00 shows a smaller slag area (see FIG 8(d)) due to a more extensive reaction between the slag and the MgO refractory. The results of the mapping analysis of Mg and Fe elements in the samples indicate that as the S/M ratio of the slag increases, the interaction between slag and the refractory material becomes more significant. This is evident through the decreasing intensity of Mg and increasing Fe intensity in the crucible. The penetration of FeO into the MgO crucible appears to be more pronounced than that of SiO₂. This phenomenon may be attributed to the ability of FeO to diffuse through and combine with the MgO monoxide solid solution.

The semi-quantitative EDS measured composition of the samples along the refractory and slag interface is provided in TABLE 4, with the compositions of the dominant components, MgO, SiO₂, and FeO, plotted in FIG 9. The experimental results indicate that the MgO concentration in most of the slags increases after the melting experiments, indicating the dissolution of MgO from the refractory into the slag (see FIG 9(a)). Conversely, the SiO₂ concentration in the slags decreases after the melting experiments due to dilution by dissolved MgO (see FIG 9(b)). There is no significant penetration of the MgO solid by the SiO₂. However, the most significant penetration of the MgO solid was by FeO, as clearly observed in the sample with an initial S/M ratio in slag of 3.00, resulting in FeO concentrations in the MgO refractory ranging from 8.4 to 27 wt.% (see FIG 9(c)).

TABLE 4 – Semi-quantitative EDS measured composition along refractory-slag interface from samples melted at 1500°C for melting time of 120 minutes with initial SiO₂/MgO ratios in slag between 1.75 and 3.00

Sample	Position												
	1	2	3	4	5	6	7	8	9	10	11	12	
Initial S/M=1.75	MgO	98.5	98.4	98.3	97.3	96.0	93.0	90.2	45.1	41.7	37.9	41.5	38.3
	SiO ₂	0.2	0.4	0.1	0.2	0.2	0.3	0.6	45.2	47.8	47.2	46.8	46.3
	Al ₂ O ₃	0.5	0.5	0.7	0.5	0.7	1.0	1.9	2.9	3.4	4.2	4.3	3.8
	CaO	0.1	0.1	0.0	0.1	0.1	0.1	0.2	0.9	1.6	2.0	0.9	4.3
	FeO	0.7	0.7	1.0	1.9	3.1	5.6	7.1	5.9	5.5	8.6	6.5	7.4
Initial S/M=2.00	MgO	98.6	98.1	98.1	96.4	95.5	92.3	54.3	37.8	34.0	32.4	32.3	31.4
	SiO ₂	0.3	0.3	0.3	0.8	0.3	0.5	42.0	50.7	49.1	48.4	49.5	52.0
	Al ₂ O ₃	0.4	0.3	0.5	0.6	0.7	1.1	1.5	3.3	5.5	6.5	6.0	4.5
	CaO	0.0	0.1	0.0	0.0	0.0	0.1	0.1	1.3	2.5	3.4	3.1	3.2
	FeO	0.6	1.2	1.1	2.2	3.4	6.0	2.1	6.9	8.9	9.4	9.1	8.9
Initial S/M=2.50	MgO	98.1	96.2	95.2	93.1	93.7	92.3	49.1	40.5	37.3	27.4	29.8	31.6
	SiO ₂	0.4	0.4	0.7	1.0	0.1	0.3	31.3	46.2	49.6	50.0	51.6	53.8
	Al ₂ O ₃	0.5	0.6	0.6	1.0	1.0	1.3	2.7	4.3	4.1	8.5	5.8	4.3
	CaO	0.1	0.4	0.1	0.7	0.0	0.1	2.4	1.9	1.5	3.6	3.0	2.3
	FeO	1.0	2.4	3.4	4.3	5.2	6.0	14.5	7.1	7.5	10.5	9.8	8.1
Initial S/M=3.00	MgO	84.1	84.8	84.7	79.3	65.4	68.6	46.0	41.1	40.1	31.2	30.9	28.9
	SiO ₂	3.7	1.0	1.3	1.4	6.5	2.2	32.6	46.0	46.6	50.2	51.4	52.5
	Al ₂ O ₃	3.0	1.0	0.6	1.1	1.6	1.4	4.9	4.2	4.1	6.5	5.1	5.9
	CaO	0.9	0.6	0.5	0.8	3.5	0.8	2.5	2.1	1.8	3.3	2.4	2.6
	FeO	8.4	12.6	13.0	17.4	23.1	27.0	14.0	6.6	7.4	8.8	10.3	10.3
REFRACTORY							OLIVINE		SLAG				

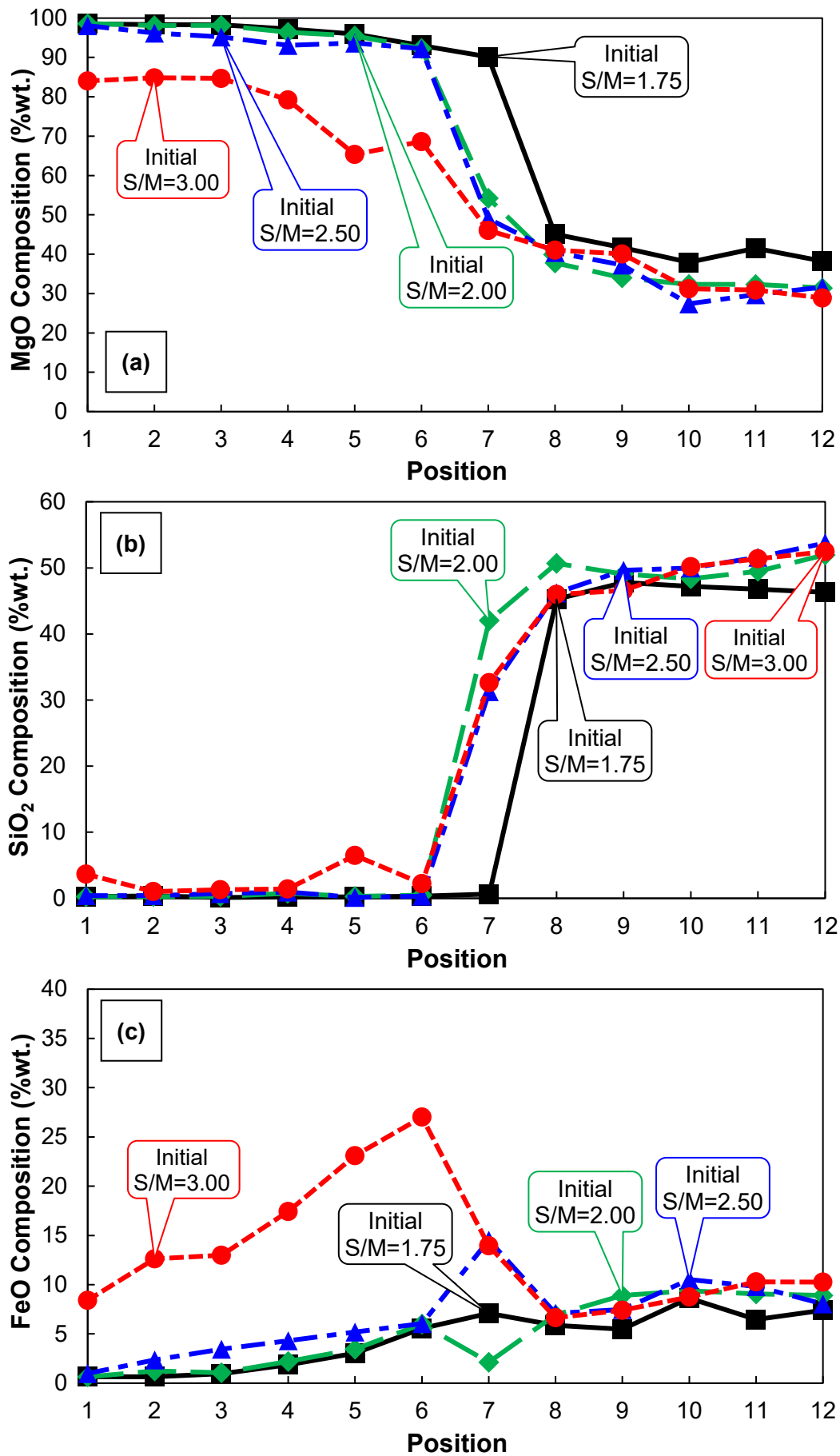


FIG 9 – Semi-quantitative compositional analysis along refractory-slag interface from samples melted at 1500°C for 120 minutes with initial SiO₂/MgO ratios in slag between 1.75 and 3.00: (a) MgO composition; (b) SiO₂ composition; and (d) FeO composition

The Corrosion Mechanism of MgO Refractory by Slag

The phases and their compositions resulting from the interaction between MgO refractory and slag at 1500°C are predicted using FactSage, as shown in FIG 10. The trends demonstrated by FactSage predictions can serve as a guide for understanding the refractory-slag interaction. In the case of sample with an initial SiO₂/MgO (S/M) ratio in slag of 2.00, the slag is entirely liquid and can accommodate MgO up to 29.4 wt.%. Further addition of MgO leads to the formation of olivine; olivine forms when the ratio of MgO to slag is 4:96. A higher ratio of MgO to slag above 30:70 leads to the stabilization of monoxide together with traces of olivine. For sample with an initial S/M ratio in slag of 3.00, the slag is fully liquid and becomes saturated with olivine at a ratio of MgO to slag of 10:90. As the ratio of MgO to slag reaches above 33:67, the slag dissipates and is replaced by monoxide with traces of olivine. In general, the phases predicted by FactSage are consistent with those observed in actual experiments.

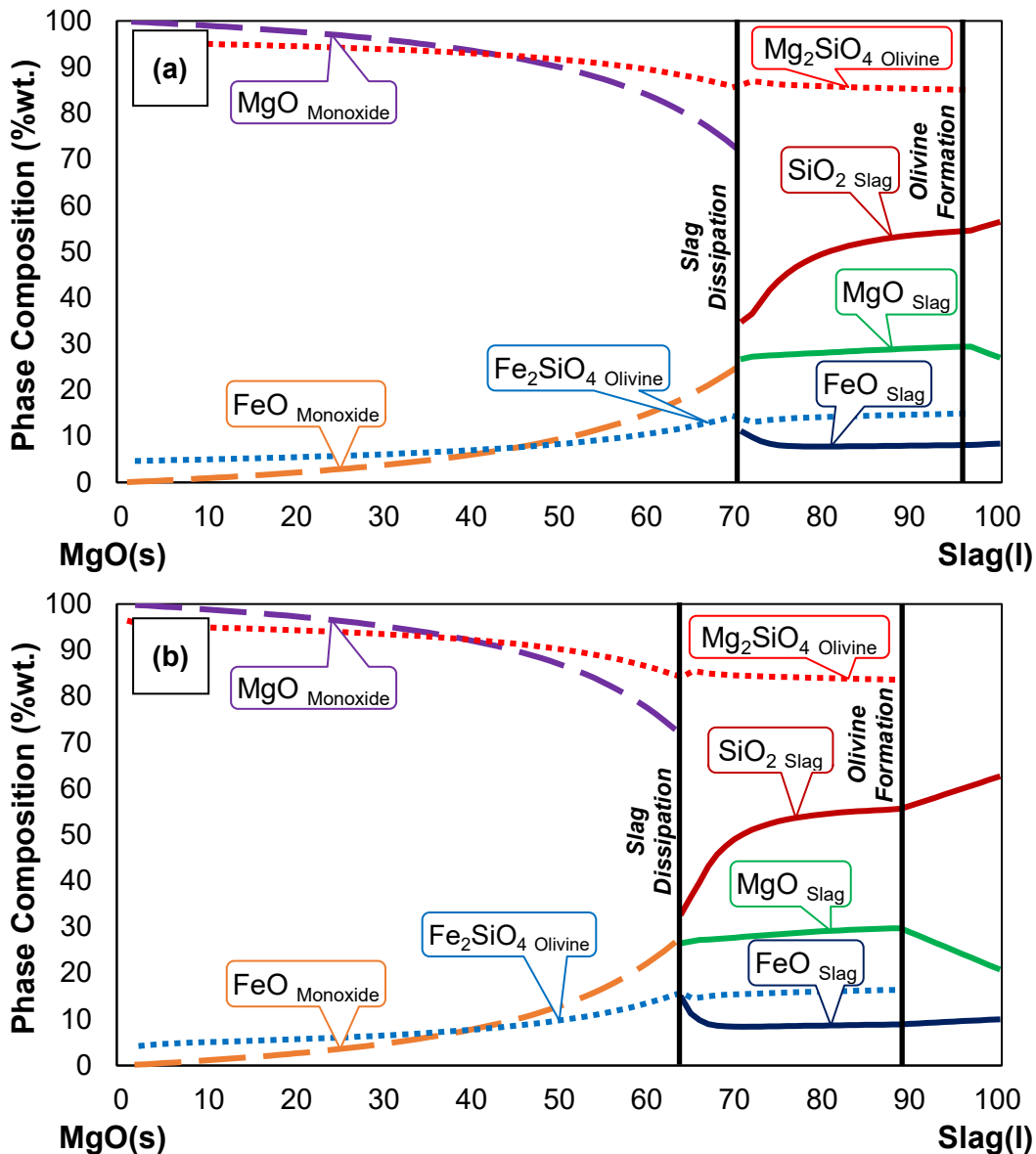


FIG 10 – FactSage calculated phase composition from interaction between MgO refractory with slag at 1500°C with initial SiO₂/MgO ratio in slag: (a) 2.00; and (b) 3.00

The sub-processes involved in refractory corrosion are depicted in FIG 11. Mass transfer of slag components such as FeO and SiO₂ (step-1) to the refractory-slag interface, and MgO (step-6) from the interface can occur due to the concentration gradient between bulk slag and the interface. Contact between FeO from the slag and MgO solid can lead to the incorporation of FeO into the

MgO solid solution (step-2); later, this can result in solid-state diffusion of FeO within the MgO refractory (step-3). On the other hand, contact between SiO₂ from the slag and MgO solid (step-4) can lead to the dissolution of MgO into the slag (step-5). Continuous dissolution of MgO into the slag can lead to the saturation of the slag by MgO, which leads to the formation of olivine (step-5b) on the surface of the MgO solid or the formation of olivine crystals within the slag (step-7). The olivine layer protects the MgO refractory from direct contact with SiO₂ but does not hinder the transfer of FeO and MgO via solid-state diffusion through the olivine layer (step-3b and 3c).

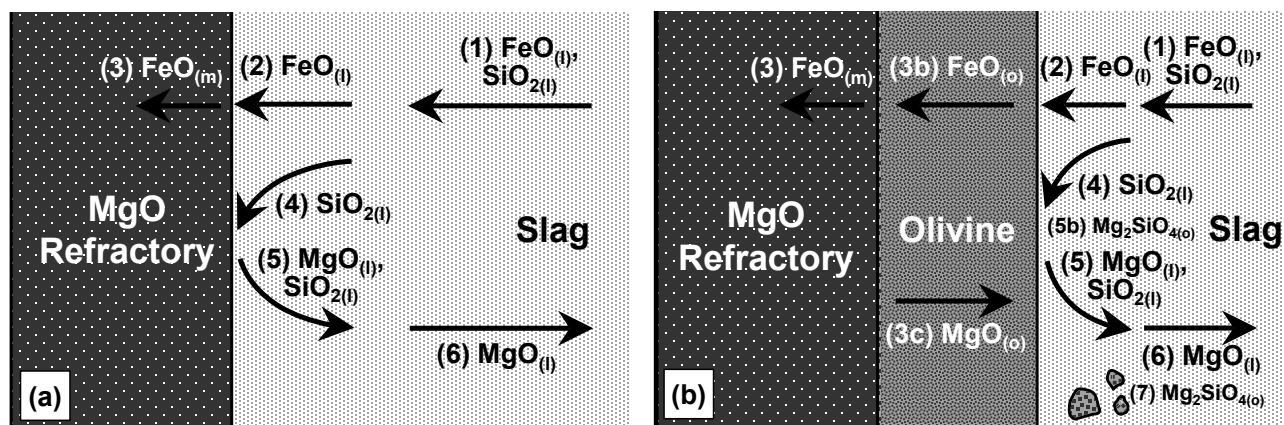


FIG 11 – Mechanism of refractory-slag interaction: (a) without olivine layer; and (b) with olivine layer

All of the sub-processes in FIG 11 take place simultaneously, and the overall refractory corrosion rate will be controlled by the slowest sub-process. The formation of the olivine layer is expected to minimize the rate of refractory corrosion since it eliminates direct contact/reaction between MgO solid and slag, creating a barrier between the two phases that can only be penetrated by slag components through relatively slow solid-state diffusion. Consequently, the composition of slag in FeNi or NPI smelting must be carefully controlled to aim for the formation of a stable, dense phase that can protect the surface of the MgO refractory and minimize the refractory and slag interaction.

CONCLUSIONS

The interaction between slag and refractory has been examined under conditions relevant to nickel laterite ore smelting. Industrial slag was replicated using synthetic slag, while the actual refractory material was replicated using a dense, pure MgO crucible. The kinetics of the slag-refractory reaction were investigated by conducting experiments at 1500°C for 5, 30, and 120 minutes using samples with selected initial S/M ratios in slag of 2.0 and 3.0 (wt./wt.) at constant CaO = 3 wt.%, Al₂O₃ = 5 wt.%, FeO = 10wt.%. The dissolution of MgO into the slag occurs at a rapid rate that within 5 to 30 minutes of melting the MgO concentration in slag increases by 2.4 wt.% and 5.7 wt.% for initial S/M ratios of 2.0 and 3.0 wt./wt., respectively. The dissolution of MgO is less rapid between 30 and 120 minutes, possibly due to a lesser driving force for MgO dissolution as the liquid approaches MgO saturation condition. The slag-refractory interaction was also studied at 1500°C for 120 minutes using initial mixtures with different initial SiO₂/MgO (S/M) ratios in slag of 1.75, 2.0, 2.5, and 3.0 (wt./wt.). All samples from the 120-minutes melting experiments exhibit areas of slag, slag-olivine mixture, and dense MgO. It was found that as the initial S/M ratio of the slag increases, the interaction between the slag and the refractory material becomes more significant, as observed from the increasing dissolution of MgO from the refractory into the slag. A higher S/M ratio in slag also results in a greater extent of solid-state diffusion of FeO into the remaining MgO grains. It is anticipated that the presence of an olivine layer can reduce the rate of corrosion on the refractory material. Therefore, it is crucial to carefully control the slag composition in FeNi or NPI smelting to ensure the formation of a stable and dense protective layer on the surface of the refractory brick.

ACKNOWLEDGEMENTS

The authors would like to acknowledge the support from PT Gunbuster Nickel Industry for providing the Scanning Electron Microscope-Energy Dispersive X-ray Spectroscopy (JCM-7000 NeoScopeTM. JEOL. Tokyo. Japan) used for the analysis of the samples in this work. The authors would also like to acknowledge the support from the Department of Mineral Sciences of the Smithsonian Institution for providing Basaltic Glass and Springwater Olivine reference materials.

REFERENCES

Crundwell, F, Moats, M, Ramachandran, V, Robinson, T and Davenport, W, 2011. *Extractive Metallurgy of Nickel, Cobalt and Platinum Group Metals* (Elsevier: Amsterdam).

Bale, C W, Bélisle, E, Chartrand, P, Deckerov, S A, Eriksson, G, Gheribi, A E, Hack, K, Jung, I H, Kang, Y B, Melançon, J, Pelton, A D, Petersen, S, Robelin, C, Sangster, J, Spencer, P and Van Ende, M A, 2016. FactSage thermochemical software and databases - 2010 - 2016, *Calphad*, 54:35–53 <www.factsage.com>

Degel, R, Kempken, J, Kunze, J and König, R, 2007. Design of a modern large capacity FeNi smelting plant, in *INFACON XI*, pp 605–620 (The Indian Ferro Alloy Producers' Association).

Gangler, J J, 1950. Some physical properties of eight refractory oxides and carbides, *Journal of the American Ceramic Society*, 33:367–374.

Huang, S, Xue, J and Wang, Z, 2017. Effect of FeO content in laterite nickel slag on the corrosion behaviour of refractory materials, in *8th International Symposium on High-Temperature Metallurgical Processing*, pp 679–688 (The Minerals, Metals & Materials Society).

Kotzé, I J, 2002. Pilot plant production of ferronickel from nickel oxide ores and dusts in a DC arc furnace, *Minerals Engineering*, 15:1017–1022.

Ruh, E and McDowell, J S, 1962. Thermal conductivity of refractory brick, *The American Ceramic Society*, 45:189–195.

Sagadin, C, Luidold, S, Wagner, C and Wenzl, C, 2016. Melting behaviour of ferronickel slags, *JOM*, 68; pp 3022–3028.

Sagadin, C, Luidold, S, Wenzl, C and Wagner, C, 2017. Evaluation of high temperature refractory corrosion by liquid $\text{Al}_2\text{O}_3\text{--Fe}_2\text{O}_3\text{--MgO--SiO}_2$, in *8th International Symposium on High-Temperature Metallurgical Processing*, pp 161–168 (The Minerals, Metals & Materials Society).

Sagadin, C, Luidold, S, Wagner, C, Spanring, A and Kremmer, T, 2018. Phase reactions between refractory and high-acidic synthetic CaO-ferronickel slag, *JOM*, 70:34–40.

Sagadin, C, Luidold, S, Wagner, C and Spanring, A, 2018. High temperature phase formation at the slag/refractory interphase at ferronickel production, in *Extraction 2018*, pp 137–147 (The Minerals, Metals & Materials Society).

Sagadin, C, Luidold, S, Wagner, C, Pichler, C, Kreuzer, D, Spanring, A, Antrekowitsch, H, Clarke, A and Clarke, K, 2021. Thermodynamic refractory corrosion model for ferronickel manufacturing, *Metallurgical and Materials Transactions B*, 52:1052–1060.

Wagner, C, Wenzl, C, Gregurek, D, Kreuzer, D, Luidold, S and Schnideritsch, H, 2017. Thermodynamic and experimental investigations of high-temperature refractory corrosion by molten slags, *Metallurgical and Materials Transactions B*, 48:119–131.

Zhang, S and Lee, W E, 2004. Direct and indirect slag corrosion of oxide and oxide-c refractories, in *VII International Conference on Molten Slags Fluxes and Salts*, pp 309–319 (The South African Institute of Mining and Metallurgy).

Zhang, S and Lee W E, 2013. Use of phase diagrams in studies of refractories corrosion, *International Materials Reviews*, 45:41–58.